Anal. Chem. **1999,** *71,* 3446−3452

Improvement in Particle Separation by Hollow Fiber Flow Field-Flow Fractionation and the Potential Use in Obtaining Particle Size Distribution

Won Ju Lee and Byoung-Ryul Min*

Department of Chemical Engineering, Yonsei University, Seou1 120-749, Korea

Myeong Hee Moon*

Department of Chemistry, Kangnung National University, Kangnung 210-702, Korea

Particle separation in hollow fiber flow field-flow fractionation (HF-FlFFF) has been greatly improved by experimentation. Flow optimization and the use of an appropriate carrier solution allow for separation of particles by HF-FlFFF to reach nearly the level of separation efficiency normally achieved by a conventional flow FFF system. The retention ratio in HF-FlFFF is confirmed to $R \cong 4\lambda$ for a highly retained component. The effect of focusing/relaxation point and the theoretical considerations of particle retention in HF-FlFFF through experimentation are discussed. The current work attempts to measure the particle size distribution of a laboratory-prepared polydisperse polystyrene latex sample, and the resulting size distribution, show a reasonable agreement with that obtained by capillary hydrodynamic fractionation. The efforts made in this work could provide possibilities for an HF-FlFFF system that can be developed into a system using a disposable and inexpensive fiber (channel in flow FFF).

Flow field-flow fractionation (FlFFF), a subtechnique of the FFF family, has been developed into a universal fractionation technique which can be applied for the separation and size characterization of particulates, water-soluble polymers, and biological macromolecules.[1−6] Like the other FFF techniques, separation in FlFFF is carried out in an open rectangular channel with the use of larminar flow. The driving force of separation in a FlFFF channel is the movement of cross-flow acting to the direction perpendicular to the axial flow. This secondary flow plays the role of an external source of field and it penetrates to and from the permeable frits which constitute the channel walls. When sample components are placed at the channel under the cross-flow, they differentially accumulate toward the one channel wall (accumulation wall) according to the degree of opposing transports of sample components caused by the diffusion. Therefore, small-sized sample components undergoing a fast diffusion are placed at a relatively fast streamline of laminar flow, and thus, they will elute earlier than the slow-diffusing large components.

The FlFFF channel described so far is of the typical rectangular design having ceramic permeable frits as channel wall material for the penetration of cross-flow, and it requires a semipermeable membrane to keep sample components from being lost. There are two main categories of rectangular flow FFF channel designs: the symmetrical channel having a pair of ceramic frits for both channel walls[1,4,7] and the asymmetrical channel with a single frit at the accumulation wall only.[3,6,8] Both channel designs require a separate relaxation process prior to the beginning of separation in order to provide equilibrium states for sample components. This is mostly achieved by stopping the channel flow (axial flow) for a symmetrical channel or by focusing two counteracting flows from both channel inlet and outlet for an asymmetrical one. To bypass the stoppage of sample migration during the relaxation process, a hydrodynamic relaxation technique is introduced by using a frit inlet for both channel designs.[9,10]

Besides these rectangular channel systems, the first experimental work on using a hollow fiber membrane as a cylindrical channel was reported by Lee et al.,[11] and this idea was suggested to be a good alternative to the conventional flow FFF channel by Doshi and Gill.[12] A series of works reported on the feasibility of using hollow fiber for the separation of polystyrene latex standards,[13,14] with the investigation of ionic strength effect of carrier

(1) Giddings, J. C.; Yang, F. J.; Myers, M. N. *Anal. Chem.* **1976**, *48*, 1126−32.
(2) Giddings, J. C. *Science* **1993**, *260*, 1456−65.
(3) Litzen, A.; Wahlund, K.-G. *J. Chromatogr.* **1989**, *476*, 413−21.
(4) Moon, M. H.; Kim, Y. H.; Park, I. *J. Chromatogr., A* **1998**, *813*, 91−100.
(5) Lee, S.; Rao, S. P.; Moon, M. H.; Giddings, J. C. *Anal. Chem.* **1996**, *68*, 1545−9.
(6) Wittgren, B.; Wahlund, K.-G.; Derand, H.; Wesslen, B. *Macromolecules* **1996**, *29*, 268−76.
(7) Ratanathanawongs, S. K.; Giddings, J. C. *Chromatographia* **1994**, *28*, 545−54.
(8) Wahlund, K.-G.; Giddings, J. C. *Anal. Chem.* **1987**, *59*, 1332−9.
(9) Liu, M.-K.; Williams, P. S.; Myers, M. N.; Giddings, J. C. *Anal. Chem.* **1991**, *63*, 2115−22.
(10) Moon, M. H.; Kwon, H.; Park, I. *Anal. Chem.* **1997**, *69*, 1436−40.
(11) Lee, H.-L.; Reis, J. F. G.; Dohner, J.; Lightfoot, E. N. *AIChE J.* **1974**, *20*, 776−84.
(12) Doshi, M. R.; Gill, W. N.; *Chem. Eng. Sci.* **1979**, *34*, 725−31.
(13) Jönsson, J. A.; Carlshaf, A. *Anal. Chem.* **1989**, *61*, 11−8.
(14) Carlshaf, A.; Jönsson, J. A. *J. Chromatogr.* **1988**, *461*, 89−93.

10.1021/ac981204p CCC: $18.00
Published on Web 07/08/1999

solution,[15] properties of fiber membrane,[16] and the overloading effect in hollow fiber flow FFF (HF-FlFFF) runs.[17] Recent attempts have been made at the separation of proteins and water-soluble polymers.[18] While hollow fiber has great potential to be used as a separation chamber in FlFFF with the advantage of instrumental simplicity and low cost for disposable use, its performance has not been thoroughly studied. Initial evaluation[13,14] showed the possibility of using a hollow fiber for the separation of particles. The resolution of particle separation using hollow fiber FlFFF in early reports is not beyond the desired level typically obtained by a rectangular channel system shown elsewhere.[4,5] It is likely that hollow fiber FlFFF, especially for particle separation, needs more studies before being used as an effective tool.

In this article, particle separation in hollow fiber flow FFF is greatly improved, nearly to the level of resolution reported with a rectangular channel system, by utilizing a carrier solution[19] that is widely known as useful for particle separation and by selecting an intermediate fiber diameter compared to the previous work.[16] Equations describing the retention ratio in HF-FlFFF are derived, and the experimental retention data are compared with the theoretical assumptions. The discussion covers the influence of injection flow rate and radial flow rate on the separation of latex mixtures, and with the possibility of fiber expansion during HF-FlFFF runs. It also demonstrates that hollow fiber flow FFF can be applied to obtain the particle size distribution (PSD) of a laboratory-prepared polydisperse polystyrene latex sample, and the resulting PSD is in good agreement with the result obtained by capillary hydrodynamic fractionation (CHDF).

THEORY

Void Time Calculation. Flow in a hollow fiber varies along the axial direction z of a fiber due to the loss of fluid through the pores, which is the radial flow shown in the enlarged view of Figure 1. The linear flow velocity, $v(r,z)$, of axial flow at any radial position r along the z axis is expressed as[20]

$$v(r,z) = 2\langle v\rangle(z)(1 - (r^2/r_f^2)) \quad (1)$$

where $\langle v\rangle(z)$ is the average linear flow velocity at any z point along the fiber and r_f is the radius of fiber. The radial flow velocity, $U(r,z)$, is given by[13]

$$U(r,z) = U(r_f,z)(2(r/r_f) - (r/r_f)^3) \quad (2)$$

In eq 2, $U(r_f,z)$ is the radial flow velocity at the fiber wall that

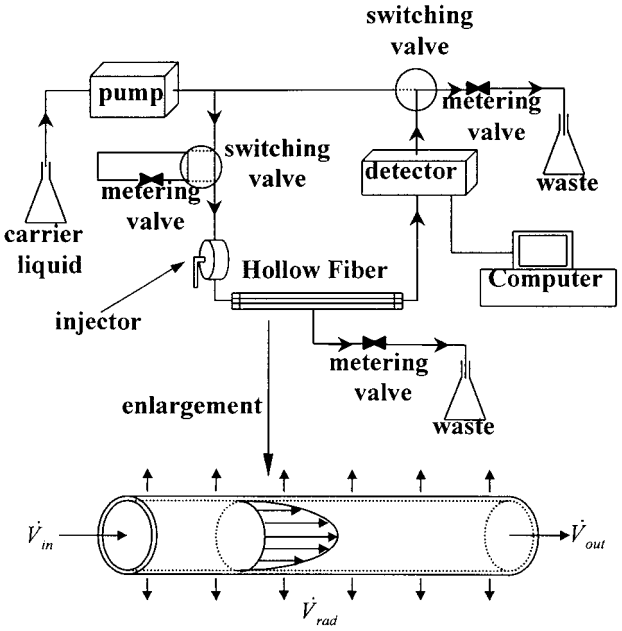

Figure 1. Schematic diagram of hollow fiber flow FFF (HF-FlFFF) system with the enlarged view of fiber representing the flow movement inside the fiber.

decreases along z as[13]

$$U(r_f,z) = U(r_f,0)\exp(-\alpha z) \quad (3)$$

where $U(r_f,0)$ is the radial flow velocity at the fiber wall and α is a constant that represents a characteristic of the fiber by $\alpha = (\eta\beta/r_f^3)^{1/2}$ (η is the viscosity of fluid liquid, β is the permeability of the fiber). In the case of a fiber pressurized during HF-FlFFF runs, radial flow velocity can be assumed as uniform along the fiber and then the $U(r_f,z)$ becomes $U(r_f)$ (In experiments using a fiber (length 24.0 cm) with permeability of 0.415 cm^3/cm^2·atm, relative error in U is about 2.0−2.3% along the entire length of the fiber.) Thus, the velocity variation in the HF-FlFFF is similar to that of the conventional asymmetrical flow FFF channel and the average flow velocity, $\langle v\rangle(z)$, at any point z along a real fiber decreases linearly as

$$\langle v\rangle(z) = \frac{\dot{V}_{in} - (z/L)\dot{V}_{rad}}{\pi r_f^2} \quad (4)$$

where $\dot{V}_{in}$ represents the volumetric flow rate at the fiber inlet, L the length of fiber, and $\dot{V}_{rad}$ the radial flow rate ($\dot{V}_{rad} = U(r_f)2\pi r_f L$). The void time in the hollow fiber is calculated as

$$t^0 = \int_0^L \frac{dz}{\langle v\rangle(z)} = \int_0^L \frac{\pi r_f^2\, dz}{\dot{V}_{in} - (z/L)\dot{V}_{rad}} = \frac{V^0}{\dot{V}_{rad}} \ln\left(\frac{\dot{V}_{in}}{\dot{V}_{out}}\right) \quad (5)$$

where V^0 represents the void volume of a fiber ($= \pi r_f^2 L$) and $\dot{V}_{out}$ is the actual flow rate of outflow that can be measured at the fiber outlet. Equation 5 is valid for both the hollow fiber and the conventional asymmetrical channel if $\dot{V}_{rad}$ is replaced with the cross-flow rate.

(15) Carlshaf, A.; Jönsson, J. A. *J. Microcolumn Sep.* **1991**, *3*, 411−6.
(16) Carlshaf, A.; Jönsson, J. A. *Sep. Sci. Technol.* **1993**, *28*, 1031−42.
(17) Carlshaf, A.; Jönsson, J. A. *Sep. Sci. Technol.* **1993**, *28*, 1191−201.
(18) Wijnhoven, J. E. G. J.; Koorn, J.-P.; Pope, H.; Kok, W. Th. *J. Chromatogr., A* **1996**, *732*, 307−15.
(19) Moon, M. H. *Bull. Korean Chem. Soc.* **1995**, *16*, 613−19.
(20) Giddings, J. C. *Unified Separation Science*; John Wiley & Sons: New York, 1991; Chapter 9.
(21) Williams, P. S.; Moon, M. H.; Giddings, J. C. *Colloids Surf. A* **1996**, *113*, 215−28.

Retention in Hollow Fiber Flow FFF. When sample components are introduced into the hollow fiber, they need to undergo a focusing/relaxation process to achieve the proper concentration profile before the separation begins. During the focusing/relaxation, sample components are distributed in radial direction as[13]

$$C = a \exp[Pe(x^2 - (x^4/4))] \tag{6}$$

where a is a constant, $x = r/r_f$, and Pe is the Peclet number defined by

$$Pe = \frac{U(r_f,z)r_f}{D} = \frac{1}{\lambda} \qquad (\text{when } U(r_f,z) \cong U(r_f)) \tag{7}$$

which is the reverse of retention parameter λ with the best approximation that radial flow velocity along a fiber is uniform. The sample zone velocity, V_p, in an FFF channel is calculated as the weight average of flow velocity by

$$V_p = \frac{\int_0^{r_f} Cv(r,z)\, dA}{\int_0^{r_f} C\, dA} \tag{8}$$

where dA is the small increment $2\pi r$ dr of cross-sectional area of fiber. Since the retention ratio, R, in FFF is represented as the ratio of particle moving velocity to the average flow velocity,[20] retention ratio in a hollow fiber flow FFF is calculated likewise as

$$R = V_p/\langle v \rangle(z) \tag{9}$$

To calculate eq 9, the exponential term of eq 6 needs to be simplified. Let us define x' as $1 - x$, x' becomes $(r_f - r)/r_f$, and the right-hand side term of the exponent in eq 6 simplifies to

$$x^2 - \frac{x^4}{4} = (1 - x')^2 - \frac{(1 - x')^4}{4} \cong \frac{3}{4} - x' = -\frac{1}{4} + x \tag{10}$$

In the above calculation, x represents for the ratio of the distance r from the fiber center to the fiber radius and x' for the ratio of the distance ($r_f - r$, the distance from the fiber wall) to the fiber radius. x' becomes a small value when the sample zone is considered, and thus, a higher order of x' such as x'^2 and x'^3 can be ignored for the calculation of the middle term in eq 10. By substituting eqs 1 and 6−8 with eq 10 into eq 9, the retention ratio, R, in hollow fiber flow FFF can be calculated as

$$R = \frac{2\int_0^{r_f}(1 - x^2)a \exp\left(\frac{1}{\lambda}\left(-\frac{1}{4} + x\right)\right)2\pi r\, dr}{\int_0^{r_f} a \exp\left(\frac{1}{\lambda}\left(-\frac{1}{4} + x\right)\right)2\pi r\, dr} = \frac{4\lambda - 12\lambda^2 + 12\lambda^3 - 12\lambda^3 e^{-1/\lambda} + 2\lambda e^{-1/\lambda}}{1 - \lambda + \lambda e^{-1/\lambda}} \tag{11}$$

where r dr is replaced with $r_f^2 x$ dx and the integration interval for x varies from 0 to 1 (r from 0 to r_f). For a very small λ ($\lambda < 0.02$)

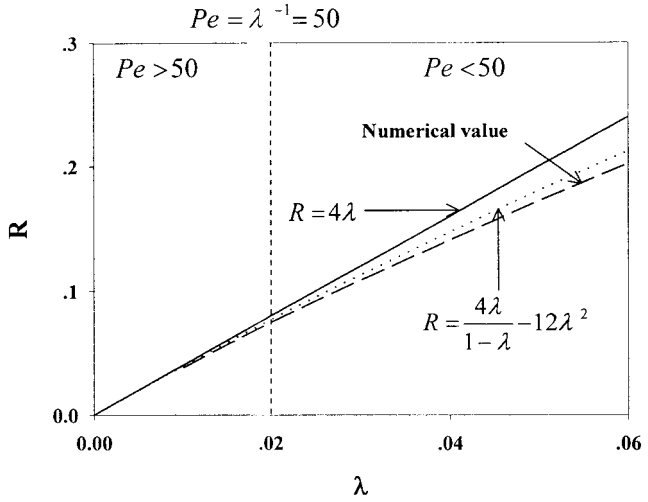

Figure 2. Variation of retention ratio R with λ according to eq 13 for solid line and eq 12 for dotted, and by the numerical integration using eqs 6−9.

or a large value of the Peclet number ($Pe > 50$), $e^{-1/\lambda}$ in the right side of eq 11 is negligibly small and eq 11 can be reduced to

$$R \cong 4\lambda/(1 - \lambda) - 12\lambda^2 \tag{12}$$

Equation 12 is the retention ratio calculated from the particle moving velocity with the consideration of radial concentration profiles of sample components in the hollow fiber. It can be further simplified in HF-FlFFF in the case of highly retained components as

$$R \cong 4\lambda \qquad (\text{where } \lambda \ll 0.02) \tag{13}$$

There is a strong restriction applied to the use of eq 13 since it is assumed that the Peclet number is constant throughout the fiber. According to the FFF theory,[1,4,5] the retention is defined as $R = t^0/t_r$ in a limited form. Thus, the retention time in a hollow fiber is calculated by using eqs 5, 7, and 13 as

$$t_r = \frac{t^0}{4\lambda} = \frac{r_f^2}{8D} \ln(\dot{V}_{in}/\dot{V}_{out}) \tag{14}$$

Equation 14 is basically the same expression to the earlier result[13] and it is dependent on the ratio of inlet flow rate to outlet flow rate. This equation is also valid only at $Pe > 50$ ($\lambda < 0.02$). (In experiments, focusing/relaxation is normally processed at or around a certain position of a fiber, $z = L_0$, and particle migration starts at L_0 when relaxation is completed. For this case, the right side of eq 14 needs to be modified as

$$t_r = \frac{r_f^2}{8D} \ln\left(\frac{\dot{V}_{in} - (L_0/L)\dot{V}_{rad}}{\dot{V}_{out}}\right) \tag{15}$$

It also applies to the calculation of void time and $\dot{V}_{in}$ on the right side of eq 5 must be replaced likewise. To check the validity of the retention ratio in a hollow fiber flow FFF, R is plotted against λ in Figure 2. The solid line represents the most simplified form

of retention ratio ($R = 4\lambda$), the dotted line for eq 12, and the broken line for the numerical integration of eq 9 with the full use of eq 6. It is shown that the deviation of retention ratio from the numerically calculated value becomes large when $\lambda > 0.02$ ($Pe < 50$). The relative errors of approximated R values from the numerical calculation at the limit of $Pe = 50$ are 3.14% for the dotted line and 7.40% for $R = 4\lambda$. For large Pe numbers ($\gg 50$), retention ratio can be treated as 4λ to a good approximation.

On the other hand, particle diameter, d, can be calculated from experimental t_r by substituting the diffusion coefficient, D, in eq 15 with $kT/3\pi\eta d$, and the rearrangement results in

$$d = \frac{8kT}{3\pi\eta r_f^2}\left\{\ln\left(\frac{\dot{V}_{in} - (L_0/L)\dot{V}_{rad}}{\dot{V}_{out}}\right)\right\}^{-1} t_r \qquad (16)$$

where $\dot{V}_{in}$ is equal to $\dot{V}_{rad} + \dot{V}_{out}$. Equation 16 can be used for the particle size calculation from an experimental fractogram of a particle sample.

EXPERIMENTAL SECTION

The HF-FlFFF system configuration is represented in Figure 1. The hollow fiber used in this work is polysulfone, having a molecular weight cutoff of 30 000, obtained from SK Chemical (Seoul, Korea). The fiber dimensions are 24 cm in length, L, and 0.80 mm for the inner diameter of dried fiber. When soaked with carrier solution and pressurized during a run, it appears to be swollen (or expanded). This phenomenon is checked by measuring the diameter of the cross section of a series of expanded membranes which are cut after freezing by being immersed into liquid nitrogen. The measured diameter of the frozen cut is 0.82 mm. The geometrical fiber volume is calculated as 0.13 mL. The fiber is encapsulated in a $^1/_8$-in. empty Teflon tube (0.078-in. i.d.) and both ends of the fiber are fixed to the inner wall of the Teflon tube with epoxy glue. A $^1/_8$-in. stainless steel union tee from Swagelok Co. (Solon, OH) is placed at the middle of the Teflon tube for radial flow exit.

The carrier solution is prepared in ultrapure water containing 0.1% FL-70 from Fisher Scientific Co. (Fair Lawn, NJ) for particle dispersion and 0.02% sodium azide as bactericide. The solution is vacuum degassed prior to use and during the run. Carrier liquid is delivered to the hollow fiber by an HPLC pump from Younglin Instrument (Seoul, Korea). Sample injection is made via a Rheodyne 7125 loop injector from Rheodyne (Cotati, CA) with an internal loop (5 μL). Followed by sample injection, the focusing/relaxation process is carried out by delivering the carrier liquid into both fiber inlet and outlet. The focusing process is accomplished with a single pump by splitting the flow into two parts (delivered to both inlet and outlet). The control of flow rates for both ends is made with the use of a model SS-SS2-VH Nupro metering valve from Nupro Co. (Willoughby, OH) which is preadjusted to give the required flow rates for focusing/relaxation. The flow rate adjustment for the outflow and radial flow is made with another metering valve. The sample particles used are polystyrene latex standards having nominal diameters of 50, 96, 155, 204, and 304 nm from Duke Scientific Co. (Palo Alto, CA). The injection amount of the standard samples is about 0.15 μg of each size. Eluted particles are monitored by a model M720 UV detector from Younglin Instrument. The detector signal is saved by a PC using the Autochro-Win data acquisition software from Younglin Instrument. For particle size distribution, a laboratory-prepared polydisperse polystyrene particle sample from Prof. Jung-Hyun Kim at the polymer laboratory in Yonsei University is tested. For comparison of particle size distribution, a model CHDF-100 capillary hydrodynamic fractionation instrument from Matec Applied Science (Hopkinton, MA) with a 5.0-μm-i.d. capillary is utilized.

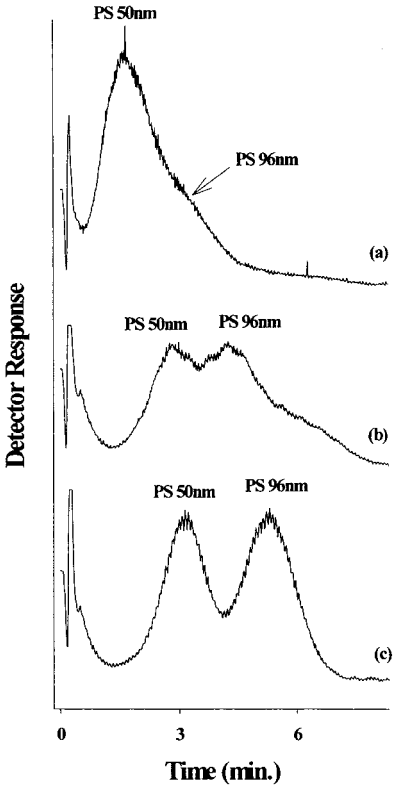

Figure 3. Elution profiles of polystyrene latex standards (diameters are marked for each peak) by varying focusing/relaxation location at (a) 0.5L, (b) 0.3L, and (c) 0.1L. Run condition for all runs is fixed at $\dot{V}_{out}/\dot{V}_{rad} = 1.40/0.10$.

RESULTS AND DISCUSSION

In field-flow fractionation, the relaxation process for sample components is a prerequisite step for obtaining good retention in a channel system prior to the separation. Since sample relaxation in HF-FlFFF is achieved by focusing/relaxation as used in asymmetrical flow FFF, a proper relaxation point selection is important in obtaining good separation and, thus the influence of focusing/relaxation point on the resolution is examined first hand. Figure 3 shows the separation of the two polystyrene standards (50 and 96 nm in diameter) obtained by varying focusing/relaxation points from 50 to 10% of the entire fiber length. All runs are obtained at $\dot{V}_{in} = 1.50$ mL/min and $\dot{V}_{out}/\dot{V}_{rad} = 1.40/0.10$ (actual flow rates in mL/min). When the focusing/relaxation is carried out at 0.5L, separation of the two components is not achieved at all. As the focusing point is moved toward the fiber inlet, each sample component shows an individual peak and a nearly baseline separation is achieved when focusing/relaxation is processed at 0.1L. Separation in Figure 3 shows a great potential for a hollow fiber system in particle separation. From this result, focusing process is accomplished at 0.1L for the entire runs. Figure 4 shows

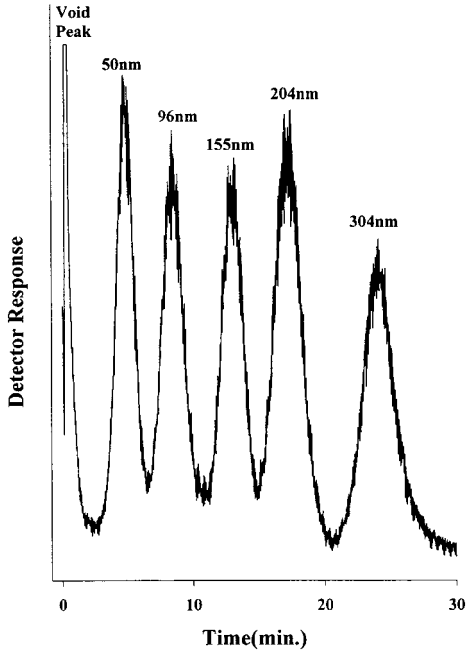

Figure 4. Separation of a polystyrene latex mixture by HF-FlFFF obtained at $\dot{V}_{out}/\dot{V}_{rad} = 1.41/0.12$.

a separation of five polystyrene mixtures obtained at $\dot{V}_{out}/\dot{V}_{rad} = 1.41/0.12$ with an injection flow rate of 0.25 mL/min. The resolving capability shown in Figure 4 is analogous to the typical runs usually obtained in a conventional symmetrical flow FFF system consisting of porous frits as the channel wall. Such resolution demonstrates that a hollow fiber can be as powerful a material for the separation and characterization of particulate materials as the rectangular frit system. In this work, the carrier solution used is water containing 0.1% FL-70 (ionic and nonionic surfactant whose components are listed in ref 19) added with 0.02% NaN_3 as a bactericide. It is thought that the ionic strength of the carrier solution plays an important role in improving the resolution since it is maintained at $I = 3.1$ mM, which falls within the optimum level for the separation of polystyrene particles in flow FFF reported earlier.[19] Another reason might be from a selection of an intermediate fiber radius (0.8-mm i.d.) compared to the earlier works[13,14] since retention of particles is significantly influenced, as suggested by eq 15.

Particle retention in HF-FlFFF is further examined by comparing experimental retention time with the theory in eq 15. To calculate the retention time from eq 15, an accurate knowledge of an exact fiber radius must be known first. Experimentally, the hollow fiber used in this work is found to be swollen in the carrier liquid when it is checked before and after use. The optical micrographs in Figure 5 are taken before (a) and after (b) a number of FFF runs. Image b in Figure 5 is obtained by cutting the frozen fiber after immediate immersion into liquid nitrogen. The radius of the fiber, r_f, is increased about 2.5% (0.41 mm from 0.40 mm). Even though the increase in radius is thought to be an artifact created by freezing of water captured in the pores of the fiber, the possibility of change in fiber radius could come from another source. Fiber expansion may occur during the run due to the system pressure. The pressure builds up about 20 psi at the current flow rates used in Figure 4 since flow adjustment is made via the needle valves at each outlet. The change in fiber

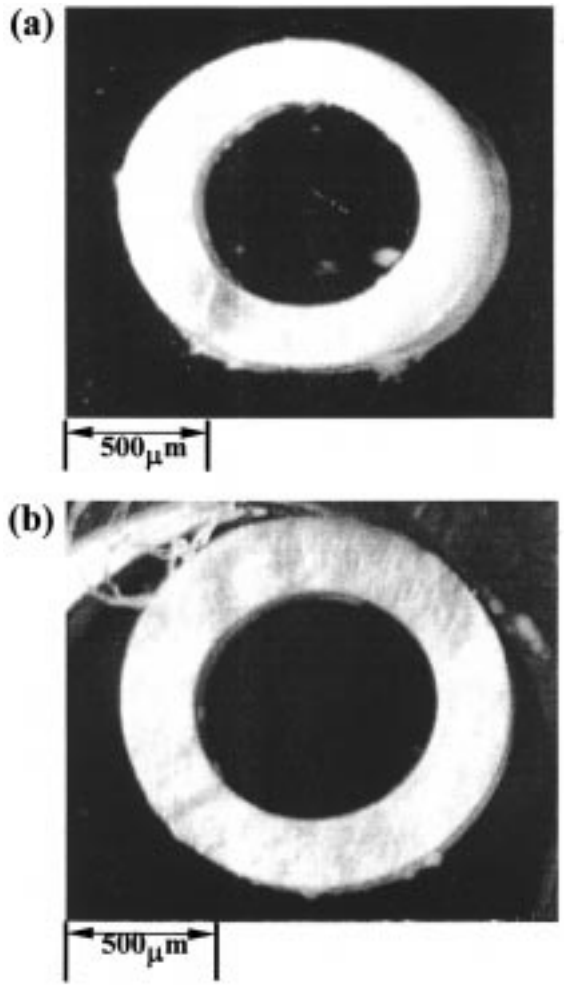

Figure 5. Optical micrographs of the hollow fiber used in this work (a) before (dry status) and (b) after HF-FlFFF run. Image b is obtained by frozen cut.

radius would result in the significant difference in retention time since t_r increases with the square of the fiber radius as suggested in eq 15. These variations are examined with PS 96-nm particles by varying the flow rate condition. Figure 6 is the plot of retention time vs radial flow rate obtained at three different axial flow rates. Experimental data points are represented as symbols. The dotted lines are the calculated retention time based on the measured fiber radius ($r_f = 0.41$ mm) of swollen fiber by using eq 15. Data points appear to lie above the theory (the dotted line) throughout the axial flow rate conditions examined in this work. It means particles retain longer than they are expected by theory. The deviations from theory may imply that there occurs fiber expansion somehow when pressure is given by the system. To estimate the change in radius, a back calculation is made to obtain an expanded radius from the experimental retention data according to eq 15, and the average radius is calculated as 0.46 mm with a relative error of about 1% for the axial flow rate conditions at 0.82, 1.11, and 1.41 mL/min. On the basis of the calibrated radius value, the expected retention time is plotted as a solid line for comparison. In Figure 6, most data points match the calculated value except the data obtained at run conditions of high radial flow rate. This deviation may arise from the influence of the steric effect when the radial flow rate is increased. It cannot be ignored that a slight variation in pressure may cause a change in fiber radius

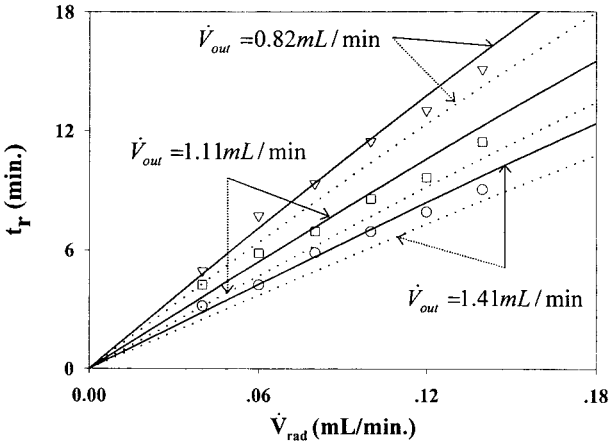

Figure 6. Plot of retention time vs radial flow rate ($\dot{V}_{rad}$) of PS 96 nm. Symbols are the experimental data points: ▽ ($\dot{V}_{out}$ = 0.82 mL/min), □ ($\dot{V}_{out}$ = 1.11 mL/min), ○ ($\dot{V}_{out}$ = 1.41 mL/min), L (24 cm), and d_f (820 μm). The dotted lines are theoretical retention times calculated from the radius (r_f = 0.41 mm), assuming that the fiber is swollen, and the solid lines are based on the calibrated radius (r_f = 0.46 mm) from the experimental data.

Table 1. Semiempirically Calculated Radius of the Hollow Fiber Used in This Work from the Theory[a]

	calculated radius (mm)		
polystyrene latex d (nm)	$\dot{V}_{in}$ = 1.13 mL/min	$\dot{V}_{in}$ = 1.52 mL/min	$\dot{V}_{in}$ = 2.19 mL/min
50	0.48	0.50	0.52
96	0.47	0.48	0.49
155	0.43	0.46	0.46
average	0.46	0.48	0.49

[a] For all runs, $\dot{V}_{rad}$ is fixed at 0.10 mL/min.

when the radial flow is varied from 0.04 to 0.14 mL/min. However, the possible increase in pressure due to the change in radial flow rate does not seem to be a critical source of fiber expansion in this case since the retention time decreases at a higher radial flow rate compared to the calculated value (the solid line).

The possibility of fiber expansion is further tested with a series of runs by using a number of standards and fiber radius is calculated for each run condition. Table 1 lists the calculated radius for each particle obtained with increasing total flux to the fiber. Even though the experiments are carried out by increasing the axial flow rate without changing the radial flow rate, fiber radius is found to increase 10−20% from the original dimension. In this calculation, the retention data of larger particles (204 and 304 nm in diameter) are not included in order to exclude any steric effect that often arises from normal flow FFF runs. The steric effect, if it occurs, results in the shift of retention into a shorter time scale. It is not quite clear whether fiber expansion is the only source of elongation in particle retention. However, the fact that retardation is systematically increased with the increase of total flux in the fiber may support the possibility of fiber expansion.

The steric influence in hollow fiber flow FFF is observed further in Figure 7. Retention time logarithms of five PS standards are plotted as symbols against the logarithms particle diameter in Figure 7. The linear lines (solid and broken) represent the semiempirical theory values based on the calibrated radius of fiber

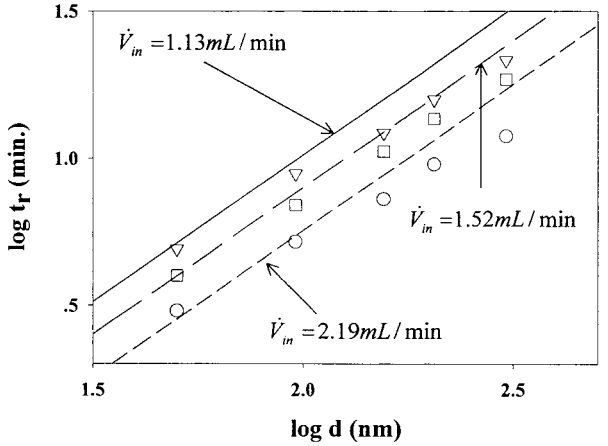

Figure 7. Plot of log t_r vs log d of PS standards obtained at different axial flow rate conditions. $\dot{V}_{rad}$ for all runs is 0.10 mL/min. Inlet flow rate of each set of data: ▽ ($\dot{V}_{in}$ = 1.13 mL/min), □ ($\dot{V}_{in}$ = 1.52 mL/min), and ○ ($\dot{V}_{in}$ = 2.19 mL/min). The linear lines are calculated on the basis of each calibrated radius from three PS standards (50, 96, 155 nm).

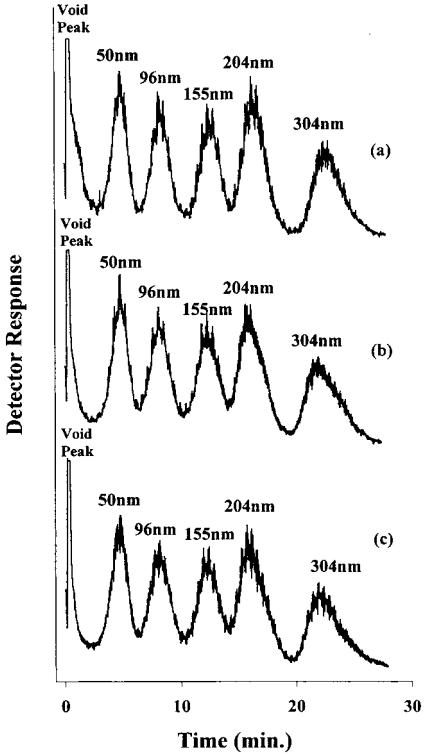

Figure 8. Influence of injection flow rate on PS separation obtained at the run condition used in Figure 4. Injection flow rates are (a) 0.25, (b) 0.50, and (c) 0.75 mL/min.

that is the average value of each run condition listed in Table 1. The data points for the large diameter size appear to deviate from the expected value, which can be explained as steric influence.

The effect of injection flow rate on the separation is tested at a run condition ($\dot{V}_{out}/\dot{V}_{rad}$ = 1.40/0.10 in actual flow rates). Figure 8 shows three fractograms of PS separation obtained at (a) 0.25, (b) 0.50, and (c) 0.75 mL/min flow rates for sample injection. Apparently, there does not seem to be a significant difference in resolution, but the 304-nm particles appear to elute earlier when the injection flow rate is used higher than 0.50 mL/min.

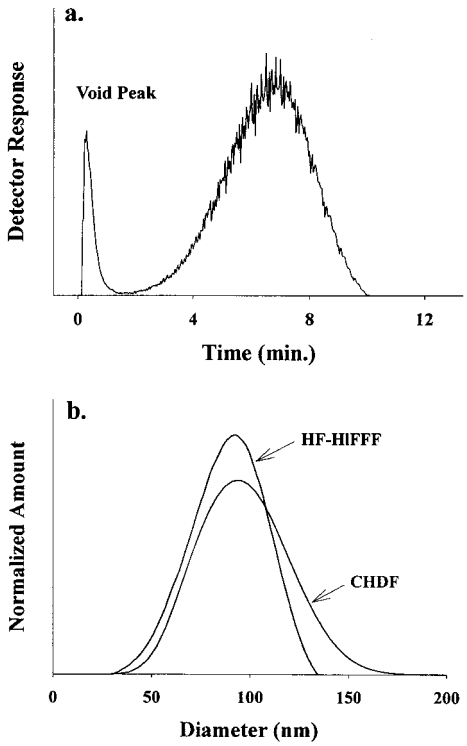

Figure 9. (a) Fractogram of a laboratory-made polydisperse polystyrene latex sample and (b) the resulting particle size distribution compared with the result of CHDF. The HF-FlFFF run is obtained at $\dot{V}_{out}/\dot{V}_{rad}$ = 1.41/0.10. CHDF result is obtained at 1.35 mL/min.

Finally, the hollow fiber flow FFF system optimized in this work is applied for the size characterization of a laboratory-prepared PS sample which is polydisperse in size distribution. Figure 9a shows a fractogram of the polydisperse PS latex sample. The run condition is $\dot{V}_{out}/\dot{V}_{rad}$ =1.41/0.10. The particle size calculation is made for the fractogram signal by using eq 16 with a calibrated fiber radius of 0.46 mm. The resulting PSD is plotted in Figure 9b and is superimposed with the PSD, the result of which is obtained by capillary hydrodynamic fractionation. The average particle diameter for the sample is measured as 92.7 nm with the standard deviation of 19.5 nm from HF-FlFFF and 95.3 nm with a standard deviation of 23.1 nm from CHDF. The HF-FlFFF result shows good agreement with the CHDF data, except for the deviation in the upper large diameter range.

CONCLUSIONS

It is shown that the separation efficiency of hollow fiber flow field-flow fractionation can be greatly enhanced by the selection of a fiber having a proper radius and by maintaining an appropriate level of ionic strength of the carrier solution with the flow optimization. The efforts made in this work demonstrate that HF-FlFFF can be potentially used as a powerful tool for particle separation and for obtaining particle size distribution. Since hollow fiber is relatively inexpensive and easily replaceable, it can be a good material as a separation chamber in flow FFF. It also provides the advantage of using a single pump that gives a simplicity in system operation and allows for a cost-effective system. To develop the hollow fiber as a disposable column in HF-FlFFF is very promising.

ACKNOWLEDGMENT

We thank Professor Jung-Hyun Kim at the polymer laboratory in Yonsei University for the supply of a laboratory-made polydisperse polystyrene sample. This work was partly supported by a Yonsei University Research Grant.

GLOSSARY

C	total concentration
d	particle diameter
d_f	fiber diameter
D	diffusion coefficient
L	fiber length
r	radial coordinate
r_f	fiber radius
t_r	retention time
U	radial flow velocity
Pe	Peclet number
v	axial flow velocity along z axis
$\dot{V}_{in}$	inlet flow rate
$\dot{V}_{out}$	outlet flow rate
$\dot{V}_{rad}$	radial flow rate
z	axial coordinate
	Greek Letters
β	permeability ($cm^3/cm^2 \cdot atm \cdot min$)
η	viscosity (g/cm s) of carrier liquid
λ	retention parameter

Received for review November 4, 1998. Accepted May 6, 1999.

AC981204P